

- ⁶A. H. Mueller, Phys. Rev. D 2, 2963 (1970).
⁷B. Hasslacher, C. S. Hsue, and D. Sinclair, Phys. Rev. D 4, 3089 (1971).
⁸C. L. Jen, K. Kang, P. Shen, and C.-I Tan, Brown University report, 1971 (unpublished).
⁹A. Bassetto, M. Toller, and L. Sertorio, Nucl. Phys. B34, 1 (1971).
¹⁰D. Z. Freedman, C. E. Jones, F. E. Low, and J. E. Young, Phys. Rev. Letters 26, 1197 (1971).
¹¹See, e.g., S. D. Drell, D. L. Levy, and T. M. Yan, Phys. Rev. D 1, 1035 (1970).
¹²H. T. Nieh and Jiunn-Ming Wang, Phys. Rev. Letters 26, 1139 (1971).
¹³T. T. Chou and C. N. Yang, Phys. Rev. D 4, 2005 (1971).

PHYSICAL REVIEW D

VOLUME 5, NUMBER 9

1 MAY 1972

Investigation of the Vertices $\pi^0\gamma\gamma$, $\eta\gamma\gamma$, and $\eta'\gamma\gamma$ with Electron-Positron Storage Rings*

J. Parisi

Laboratoire de Physique Générale, Faculté des Sciences de l'Université VI de Paris, Paris, France

and

P. Kessler

Laboratoire de Physique Atomique, Collège de France, Paris, France

(Received 5 November 1971)

We study the creation of pseudoscalar particles (π^0 , η , η') through photon-photon collisions in electron-positron storage rings, according to the original idea of Low. We here suggest that the outgoing electron and positron should be detected in their nearly forward directions, in coincidence with two photons (from the decay of the pseudoscalar particle produced) emitted at large angle. Assuming realistic experimental cutoffs, we show that (a) the integrated cross sections should be high enough to justify experiments of this type with future electron-positron storage rings of beam energy 1–3 GeV and luminosity $\sim 10^{32}$ cm⁻²sec⁻¹; (b) the background due to double bremsstrahlung is made negligible through our choice of the kinematic conditions. The interest of these experiments is discussed, and details of calculation are given.

I. INTRODUCTION

As early as 1960, Low¹ suggested the investigation of the $\pi^0\gamma\gamma$ vertex by using two colliding virtual-photon spectra in electron-electron or electron-positron colliding beams. Obviously, this idea can be extended to the $\eta\gamma\gamma$ and $\eta'\gamma\gamma$ vertices. With respect to other types of experiment based upon the Primakoff effect,² the procedure considered here has the advantage that it does not involve any hadronic background. On the other hand, such an investigation would be part of the general study of photon-photon collisions in e^-e^- or e^-e^+ colliding beams, suggested in 1960³ and made popular through a series of theoretical papers since 1969.⁴⁻⁸

We suggest considering the same experimental scheme as defined in previous papers^{5,8,9} for studying $e^-e^+ \rightarrow e^-e^+A^-A^+$, the charged particles A^-, A^+ being replaced here by the two photons from the decay $X \rightarrow 2\gamma$ ($X = \pi^0, \eta, \text{ or } \eta'$). This means that the outgoing electron and positron should be detected at very small angles (a few milliradians)¹⁰

with respect to their incident directions, in coincidence with both photons emitted at large angle with respect to the beam axis.

The leading Feynman diagram for the process $e^-e^+ \rightarrow e^-e^+X \rightarrow e^-e^+\gamma\gamma$ is shown in Fig. 1(a). [The other diagram of the same order in quantum electrodynamics (QED), where two timelike photons are exchanged, gives a completely negligible contribution, since it involves at least one extremely high q^2 value.] The corresponding kinematic scheme is shown in Fig. 2.

The selection of extremely small scattering angles for the e^\pm particles ensures that the four-momenta squared (q^2, q'^2) of both spacelike photons exchanged in the diagram of Fig. 1(a) also remain very small ($\sqrt{q^2}$ is at most of the order of a few MeV for beam energies of a few GeV), so that one may assume that the electromagnetic form factors $F(q^2, q'^2)$ involved are practically equal to $F(0, 0)$. Thus, in principle, a quite precise measurement of the coupling constants for the various $X\gamma\gamma$ vertices [or, equivalently, of the decay widths $\Gamma(X \rightarrow 2\gamma)$] can be performed.

The main problems are: (a) counting rates; (b) rejection of the background. This background is represented here by the double-bremsstrahlung process $e^-e^+ \rightarrow e^-e^+\gamma\gamma$, the leading term of which is given by the Feynman diagram of Fig. 1(b) – where the right-hand vertex corresponds to a double Compton effect in pure QED – plus the symmetric one derived from it by interchanging the left-hand and right-hand vertex. This type of diagram should indeed predominate (because of the “almost real” photon exchanged) over that where one photon is emitted at either vertex.

In the following sections, we will show that

(a) assuming realistic experimental conditions, i.e., cutoffs on various angles and energies, the cross sections predicted are still high enough to ensure reasonable counting rates in future experiments with e^-e^+ storage rings of beam energy 1–3 GeV and luminosity $\sim 10^{32} \text{ cm}^{-2} \text{ sec}^{-1}$;

(b) the double-bremsstrahlung contribution is negligible under these kinematic conditions.

In conclusion, we shall briefly discuss the physical interest of this study. Details of our calculations will be given in an appendix.

II. INTEGRATED CROSS SECTIONS FOR $e^-e^+ \rightarrow e^-e^+X \rightarrow e^-e^+\gamma\gamma$ WITH VARIOUS CUTOFF PARAMETERS

As in Ref. 9, we assume from the start that realistic experimental cutoff parameters are introduced, namely:

- (i) a maximal scattering angle θ_{\max} for both e^\pm particles, such that (see Fig. 2) $\theta, \theta' \leq \theta_{\max}$;
- (ii) a minimal emission angle ψ_{\min} for both photons, such that (see Fig. 2) $\psi_{\min} \leq \psi, \psi' \leq \pi - \psi_{\min}$;
- (iii) a minimal relative energy loss χ_{\min} for both the scattered electron and positron, such that $\chi_{\min} \leq \chi, \chi'$, where we define

$$\chi = (E_0 - E)/E_0, \quad \chi' = (E_0 - E')/E_0,$$

calling E_0 the beam energy and E, E' the respective energies of the electron and positron after scattering;

- (iv) a maximal relative energy loss χ_{\max} for both e^\pm particles, such that $\chi, \chi' \leq \chi_{\max}$.

In addition, the following parameters were used in our calculations:

- (1) partial decay rates $\Gamma(X \rightarrow 2\gamma)$: 11 eV for $X = \pi^0$,¹¹ 1 keV for $X = \eta$,¹¹ 5 keV for $X = \eta'$ (assuming simply that this rate is approximately proportional to m_X^3),
- (2) branching ratios $\Gamma(X \rightarrow 2\gamma)/\Gamma(X \rightarrow \text{total})$: 100% for π^0 , 40% for η ,¹² 10% for η' ,¹³
- (3) masses m_X of X : 135 MeV for π^0 ; 549 MeV for η ; 958 MeV for η' .

The calculation method used was a type of dou-

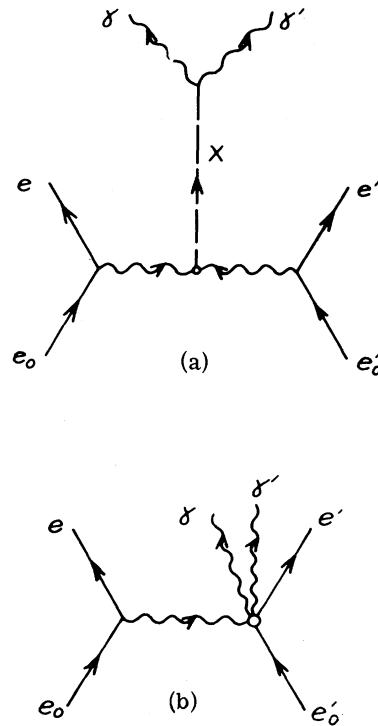


FIG. 1. (a) Main Feynman diagram for the process $e^-e^+ \rightarrow e^-e^+X \rightarrow e^-e^+\gamma\gamma$ ($X = \pi^0, \eta, \text{ or } \eta'$). (b) Leading diagram (under the conditions defined) for the double-bremsstrahlung process $e^-e^+ \rightarrow e^-e^+\gamma\gamma$.

ble Williams-Weizsäcker approximation we have developed on the basis of the generalized helicity method.¹⁴ In this approximation, the error involved should not be higher than a few percent under the conditions defined, i.e., θ_{\max} of the order of a few milliradians (see Appendix, part 1).

Figure 3 shows, for (a) $X = \pi^0$, (b) $X = \eta$, (c) $X = \eta'$, the energy behavior of the integrated cross section, predicted under the following conditions: $\theta_{\max} = 4 \text{ mrad}$, $\chi_{\max} = 70\%$, $\chi_{\min} = 2.5 \text{ or } 5\%$, $\psi_{\min} = 30^\circ \text{ or } 45^\circ$. For comparison, we also show the curves (already given in Ref. 8) representing $\sigma(E_0)$ for $e^-e^+ \rightarrow e^-e^+X$ with no other cutoff than $\theta_{\max} = 4 \text{ mrad}$.

Since no invariant mass lower than $2\chi_{\min}E_0$ can

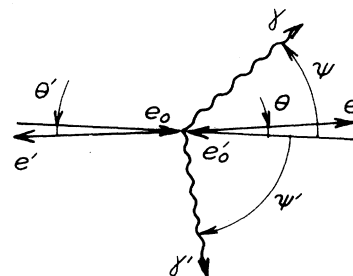


FIG. 2. Kinematic scheme corresponding to Figs. 1(a) and 1(b) (for simplicity, azimuthal angles are left out).

be produced, it is obvious that all cross sections must vanish above the value $E_0 = m_X / (2\chi_{\min})$. This fact implies in particular that the π^0 production experiment must be done at relatively low beam energy.

In Table I we show the numerical values, corresponding to the curves of Fig. 3, for $\sigma(E_0)$ at

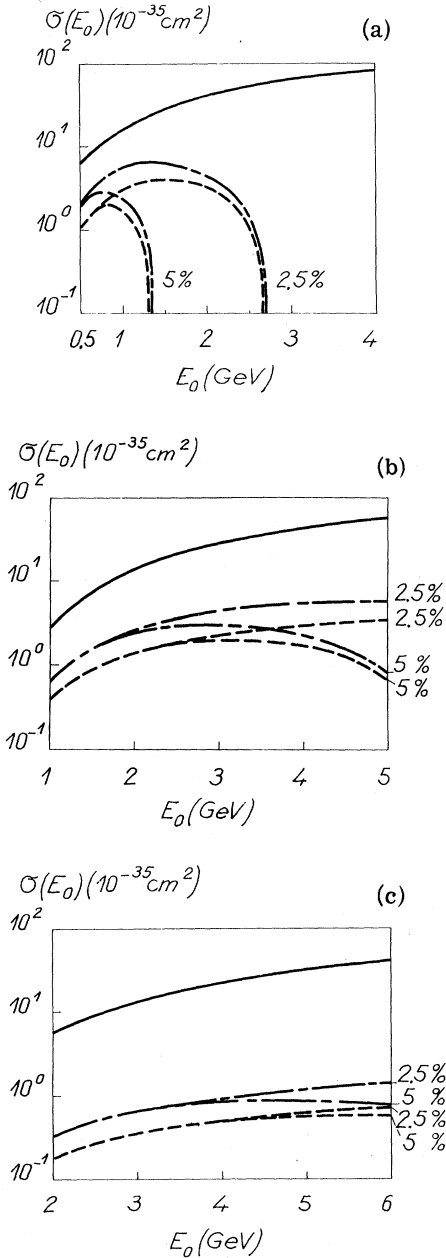


FIG. 3. Integrated cross section vs beam energy, for the process $e^-e^+ \rightarrow e^-e^+X \rightarrow e^-e^+\gamma\gamma$ at $\theta_{\max} = 4$ mrad, $\chi_{\max} = 70\%$, $\chi_{\min} = 2.5\%$ or 5% , and ——— $\psi_{\min} = 30^\circ$; - - - - $\psi_{\min} = 45^\circ$. The full curve represents the integrated cross section for $e^-e^+ \rightarrow e^-e^+X$ at $\theta_{\max} = 4$ mrad, with no other cutoffs. (a) $X = \pi^0$; (b) $X = \eta$; (c) $X = \eta'$.

$E_0 = 1, 2, 3$ GeV. It can be seen that, assuming a luminosity of $\sim 10^{32} \text{ cm}^{-2} \text{ sec}^{-1}$, reasonably large counting rates can be achieved (more than one count per hour), if – for instance – the following beam energies are used: 1 GeV for π^0 , 2 GeV for η , and 3 GeV for η' production.¹⁵

Since in actual experiments the cutoff parameters may have somewhat different values, we study, in Figs. 4, 5, 6, and 7, the effect of the variation of each of these parameters, all others being kept constant and the energy being fixed ($E_0 = 1$ GeV for π^0 , 2 GeV for η , and 3 GeV for η'). [Numerical values for $\sigma(\theta_{\max})$ are also given in Table II.] It can be noticed that none of these variations has a very violent effect on the integrated cross section, except that

(a) in the π^0 case, since – as mentioned above – no invariant mass lower than $2\chi_{\min}E_0$ can be produced, the cross section tends to vanish, when χ_{\min} approaches (from below) the value $m_{\pi^0}/(2E_0)$;

(b) in the η and η' cases, conversely, the cross section tends to vanish, when χ_{\max} approaches (from above) the value $m_X/(2E_0)$.

III. BACKGROUND SUPPRESSION

In Fig. 8, we show the energy behavior of the integrated cross section for the leading term [the diagram of Fig. 1(b), plus the symmetric one] of double bremsstrahlung; it was calculated according to part 2 of the Appendix.¹⁶ The cutoff parameters chosen were $\theta_{\max} = 4$ mrad, $\chi_{\max} = 70\%$, $\chi_{\min} = 2.5\%$, and $\psi_{\min} = 30^\circ$. The 2γ invariant mass was integrated over, in the three cases considered ($X = \pi^0, \eta, \eta'$), between $m_X - \Delta m$ and $m_X + \Delta m$, assuming that a reasonable value for Δm would be 100 MeV.

One notices that, in all three cases, the integrated cross section of this background remains lower than 10^{-40} cm^2 , so that the contamination due to it may be neglected.

We must remark that we have not calculated the contribution of the interference between the Feynman diagrams of Figs. 1(a) and 1(b), i.e., the main process and the background process. However, from the values obtained separately for both diagrams, and from the small widths of the particles X , we may infer that also this interference term should be systematically several orders of magnitude smaller (under the conditions chosen) than the term of interest.

In order to see how sensitive the contamination is to variations in the cutoff parameters, we have to compare formulas (A25) and (A16) of the Appendix. We notice that the background term, as compared to the main term, shows a much sharper decrease with increasing ω ; that means that the

TABLE I. $\sigma(E_0)$ in 10^{-35} cm² for the process $e^-e^+ \rightarrow e^-e^+X \rightarrow e^-e^+\gamma\gamma$ ($X = \pi^0, \eta, \eta'$) with $\theta_{\max} = 4$ mrad, $\chi_{\max} = 70\%$, $\chi_{\min} = 2.5\%$ or 5% , $\psi_{\min} = 30^\circ$ or 45° .

	χ_{\min}	ψ_{\min}	$X = \pi^0$		$X = \eta$		$X = \eta'$	
			30°	45°	30°	45°	30°	45°
$E_0 = 1$ GeV	2.5%		5.57	3.06	0.65	0.39	0.10	0.07
	5%		2.21	1.68	0.65	0.39	0.10	0.07
$E_0 = 2$ GeV	2.5%		4.26	3.22	2.60	1.36	0.32	0.18
	5%		0.00	0.00	2.46	1.36	0.32	0.18
$E_0 = 3$ GeV	2.5%		0.00	0.00	4.29	2.21	0.65	0.34
	5%		0.00	0.00	2.94	1.98	0.64	0.34

contamination will be further reduced if one chooses a higher value of χ_{\min} .

As to the angular dependence of the contamination, one may remark the following:

(a) Formula (A25), as compared with (A16), shows that the ratio background/(main term) will strongly increase with decreasing ψ_{\min}^* (or ψ_{\min}).

(b) This ratio will also increase with increasing θ_{\max} . (This remark is connected with the fact that, in the background, only one of the outgoing e^\pm particles is sharply peaked around 0° .)

We may take account of both (a) and (b) by stating the following condition for keeping the contamination small: $\psi_{\min} \gg \theta_{\max}$. Qualitatively, this condition is easily justified as follows: If ψ_{\min} and θ_{\max} were allowed to become comparable, more "almost on-shell" particles would appear in the double-bremsstrahlung diagrams, enhancing substantially the contribution of those diagrams.

This consideration is illustrated by Fig. 9 for the case of π^0 production (the cases of η and η' production are qualitatively similar; see Ref. 17). Here the ratio R between the contribution of the diagram of Fig. 1(b) (plus the symmetric diagram) and that of the diagram of Fig. 1(a) is plotted against ψ_{\min} for various values of θ_{\max} , all other parameters being kept constant.

It should be noticed that these curves give rather

a lower limit for the contamination, because (a) for values of θ_{\max} higher than a few milliradians, the latter process should have its contribution reduced by electromagnetic form factors (which were not included in our calculations); (b) for ψ_{\min} and θ_{\max} taking comparable values, the background calculation should include also that double-bremsstrahlung diagram where one photon is emitted at either vertex.

This background study leads us in particular to recommend that the following simplified types of experiment should be ruled out:

- (1) measurement of the decay photons alone [in this case, the significance of the experiment would be further reduced by the electromagnetic form factors coming in, in the sense that it would no longer be a measurement of $\Gamma(X \rightarrow 2\gamma)$];
- (2) measurement of the scattered e^\pm particles alone, X being identified through its missing mass.

CONCLUSION

This type of electron-positron colliding-beam experiment, based on the simultaneous measurement of the two scattered e^\pm particles in their nearly forward directions and of two decay photons emitted at large angle, should allow a more ac-

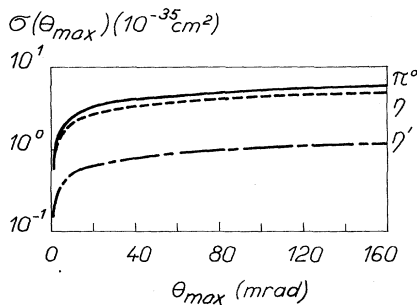


FIG. 4. Integrated cross section vs θ_{\max} , for the process $e^-e^+ \rightarrow e^-e^+X \rightarrow e^-e^+\gamma\gamma$ at $\chi_{\max} = 70\%$, $\chi_{\min} = 5\%$, $\psi_{\min} = 45^\circ$. ——— $X = \pi^0$, $E_0 = 1$ GeV. - - - - $X = \eta$, $E_0 = 2$ GeV. - - - - $X = \eta'$, $E_0 = 3$ GeV.

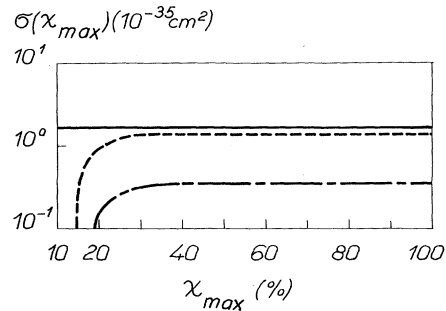


FIG. 5. Integrated cross section vs χ_{\max} for the process $e^-e^+ \rightarrow e^-e^+X \rightarrow e^-e^+\gamma\gamma$ at $\theta_{\max} = 4$ mrad, $\chi_{\min} = 5\%$, $\psi_{\min} = 45^\circ$. ——— $X = \pi^0$, $E_0 = 1$ GeV. - - - - $X = \eta$, $E_0 = 2$ GeV. - - - - $X = \eta'$, $E_0 = 3$ GeV.

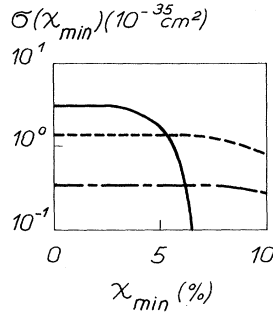


FIG. 6. Integrated cross section vs χ_{\min} for the process $e^-e^+ \rightarrow e^-e^+X \rightarrow e^-e^+\gamma\gamma$ at $\theta_{\max}=4$ mrad, $\chi_{\max}=70\%$, $\psi_{\min}=45^\circ$. — $X=\pi^0$, $E_0=1$ GeV. - - - $X=\eta$, $E_0=2$ GeV. - · - $X=\eta'$, $E_0=3$ GeV.

curate determination of $\Gamma(\pi^0 \rightarrow 2\gamma)$ and $\Gamma(\eta \rightarrow 2\gamma)$, with respect to present values obtained through the Primakoff effect. It should also allow a measurement of $\Gamma(\eta' \rightarrow 2\gamma)$ which is still unknown.

In the η' case, one may be tempted to think that it would be preferable to use one of the more important decay channels, rather than the relatively weak channel $\eta' \rightarrow 2\gamma$, in order to identify the η' particle. However, all channels with high branching ratios involve more than two final particles, and thus the analysis would become considerably more difficult.

To conclude, let us mention an interesting feature – from the phenomenological point of view – of the vertices $X\gamma\gamma$ considered here. Keeping one photon real or “almost real,” the electromagnetic form factor $F(q^2, q'^2)$ for this type of vertex becomes $F(q^2, 0) = F(q^2)$. This form factor has the property that it can be measured, at least in principle, in any region of q^2 , except for an extremely small timelike interval ($0 < q^2 < 4m_e^2$). The corresponding experiments would be the following:

- (a) $e^-e^+ \rightarrow X\gamma$ ($q^2 \geq m_X^2$, timelike),

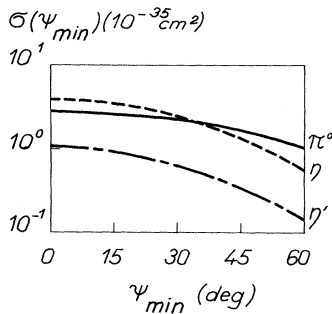


FIG. 7. Integrated cross section vs ψ_{\min} for the process $e^-e^+ \rightarrow e^-e^+X \rightarrow e^-e^+\gamma\gamma$ at $\theta_{\max}=4$ mrad, $\chi_{\max}=70\%$, $\chi_{\min}=5\%$. — $X=\pi^0$, $E_0=1$ GeV. - - - $X=\eta$, $E_0=2$ GeV. - · - $X=\eta'$, $E_0=3$ GeV.

TABLE II. $\sigma(\theta_{\max})$ in 10^{-35} cm^2 for the process $e^-e^+ \rightarrow e^-e^+X \rightarrow e^-e^+\gamma\gamma$ ($X=\pi^0, \eta, \eta'$) with $\chi_{\max}=70\%$, $\chi_{\min}=5\%$, $\psi_{\min}=45^\circ$.

θ_{\max} (mrad)	$X=\pi^0$ $E_0=1$ GeV	$X=\eta$ $E_0=2$ GeV	$X=\eta'$ $E_0=3$ GeV
1	0.75	0.59	0.16
4	1.68	1.36	0.34
7	2.15	1.76	0.44
10	2.49	2.05	0.50
20	3.22	2.66	0.64
40	4.04	3.35	0.81
60	4.55	3.79	0.91
80	4.94	4.12	0.99
100	5.25	4.39	1.05
120	5.51	4.61	1.10
140	5.74	4.80	1.14

- (b) $X \rightarrow \gamma e^-e^+$ (or $\gamma \mu^- \mu^+$) ($4m_e^2 \leq q^2 \leq m_X^2$, timelike),

- (c) $e^-e^+ \rightarrow e^-e^+X$ ($q^2 \lesssim 0$, spacelike).

Colliding-beam experiments of type (a) were performed recently in the region of the vector mesons.¹⁸ Reaction (b) has been studied experimentally, in the case $X=\pi^0$, for a long time already.¹⁹

To study the process (c) in the region of large spacelike q^2 values, a variant of the experiment discussed in this paper may be considered²⁰: One of the e^\pm particles would still be detected in its nearly forward direction, whereas the other one would be measured at large angle. This suggestion will be discussed in full detail in our next paper.²¹

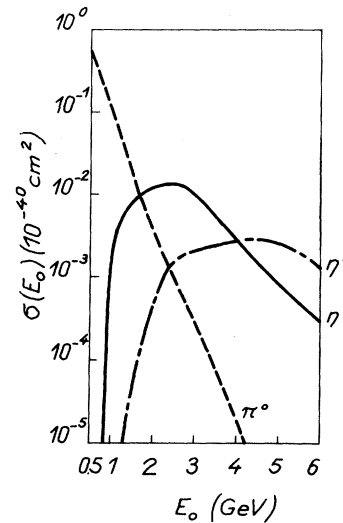


FIG. 8. Integrated cross section vs beam energy for the double-bremsstrahlung process $e^-e^+ \rightarrow e^-e^+\gamma\gamma$ at $\theta_{\max}=4$ mrad, $\chi_{\max}=70\%$, $\chi_{\min}=2.5\%$, $\psi_{\min}=30^\circ$. The $\gamma\gamma$ invariant mass was integrated over between $m_X - 100$ MeV and $m_X + 100$ MeV ($X=\pi^0, \eta, \text{ or } \eta'$).

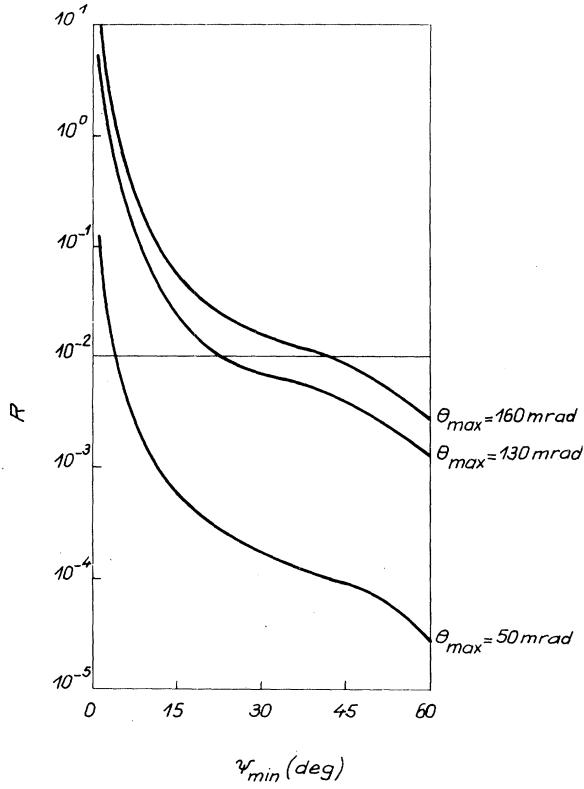


FIG. 9. Ratio between the background process [double bremsstrahlung, Fig. 1(b)] and the process of interest [$e^-e^+ \rightarrow e^-e^+X \rightarrow e^-e^+\gamma\gamma$, Fig. 1(a)], as a function of ψ_{\min} , at various values of θ_{\max} ; $\chi_{\max} = 70\%$, $\chi_{\min} = 5\%$. Here $X = \pi^0$, $E_0 = 1$ GeV. The $\gamma\gamma$ invariant mass was integrated over, for the background process, between $m_{\pi^0} - 100$ MeV and $m_{\pi^0} + 100$ MeV.

ACKNOWLEDGMENTS

The authors are deeply indebted to Professor M. Morand and Professor F. Perrin for their interest and help. They are grateful to Professor P. Waloschek and Professor J. Haissinski for very detailed discussions on the experimental conditions considered in this work. They also wish to express their gratitude to N. Arteaga-Romero, E. Calva-Tellez, and A. Jaccarini for their collaboration on various questions treated in the Appendix of this paper. Finally, they wish to thank J. P. Jobez and P. Bonierbale for their technical cooperation.

APPENDIX: DETAILS OF CALCULATION

1. Main Term

To obtain the cross section for $e^-e^+ \rightarrow e^-e^+X$, our treatment is similar to that used in the Appendix of Ref. 8, but slightly simpler. The generalized helicity method¹⁴ allows us to write

$$d\sigma = (4\pi\alpha)^4 dC D, \quad (\text{A1})$$

with

$$dC = \frac{1}{32\pi^4} \frac{m^8}{E_0^4} \frac{d\omega}{\omega} d\Phi d\tau d\tau', \quad (\text{A2})$$

$$D = (512m^8\tau'^2\tau'^2)^{-1} \times (I_{++}I'_{++} - I_{+-}I'_{+-} \cos 2\phi) |j|^2, \quad (\text{A3})$$

where we use the following symbols: m is the electron mass; E_0 is the beam energy; ω is the lab energy of the left-hand virtual photon; Φ is the azimuthal angle between the outgoing electron and positron in the lab frame, with respect to the beam axis; $\tau = |q^2|/(4m^2)$, and $\tau' = |q'^2|/(4m^2)$, q^2 and q'^2 being the squared four-momenta of the left-hand and right-hand virtual photon, respectively; ϕ is the azimuthal angle between the outgoing e^\pm particles, with respect to the $\gamma\gamma$ collision axis, in the $\gamma\gamma$ center-of-mass frame; I_{++}, I_{+-} are matrix elements of the left-hand virtual photon's polarization matrix, defined in the $\gamma\gamma$ c.m. frame, with respect to the $\gamma\gamma$ collision axis; I'_{++}, I'_{+-} are defined in an entirely similar way for the right-hand virtual photon; finally, j is the amplitude of the process $\gamma\gamma \rightarrow X$.

The small transfer (Williams-Weizsäcker type) approximation we use shows up in the following way:

(a) The exact expression of $\cos\phi$ is easily shown to be given by the relation

$$\begin{aligned} 2(E^{*2} - m^2)^{1/2}(E'^{*2} - m^2)^{1/2} \sin\theta^* \sin\theta'^* \cos\phi \\ = 2E^*E'^* - 2(E^{*2} - m^2)^{1/2}(E'^{*2} - m^2)^{1/2} \cos\theta^* \cos\theta'^* \\ + 2m_X(E^* + E'^*) + m_X^2 - 4E_0^2 + 2m^2, \end{aligned} \quad (\text{A4})$$

where m_X is the mass of X ; E^* and E'^* are the energies of the outgoing electron and positron in the $\gamma\gamma$ c.m. frame; and θ^*, θ'^* are, in that frame, their emission angles with respect to the $\gamma\gamma$ collision axis. Noticing that the ingoing and outgoing e^\pm particles are extreme-relativistic (in both the lab frame and the $\gamma\gamma$ c.m. frame) and that (under the kinematic conditions imposed) we have $|q^2| \ll m_X^2$, $|q'^2| \ll m_X^2$, we obtain, when expressing $E^*, E'^*, \theta^*, \theta'^*$ in the lab frame,

$$\begin{aligned} \cos\phi = \left[1 + O\left(m^2, \frac{q^2}{m_X^2}, \frac{q'^2}{m_X^2}\right) \right] \cos\Phi \\ + O\left(m^2, \frac{q^2}{m_X^2}, \frac{q'^2}{m_X^2}\right). \end{aligned} \quad (\text{A5})$$

Integrating over Φ , we then get

$$\int (\cos 2\phi) d\Phi = 4\pi O\left(m^2, \frac{q^2}{m_x^2}, \frac{q'^2}{m_x^2}\right). \quad (\text{A6})$$

Thus the polarization term on the right-hand side of (A3) vanishes after integration over Φ , once we neglect terms in m^2 , $|q^2/m_x^2|$, $|q'^2/m_x^2|$.

(b) Neglecting again terms in m^2 , $|q^2/m_x^2|$, $|q'^2/m_x^2|$, we get

$$I_{++} = [(1 + 2\tau_{\min})/\tau_{\min}] \tau - 1 \quad (\text{A7})$$

and an analogous expression for I'_{++} .

(c) Neglecting once more terms in $|q^2/m_x^2|$ and $|q'^2/m_x^2|$, the amplitude j is connected with the decay width $\Gamma(X \rightarrow 2\gamma)$ through the relation

$$|j|^2 = (\pi\alpha^2)^{-1} m_x \Gamma(X \rightarrow 2\gamma). \quad (\text{A8})$$

Using (A1)–(A3) and (A6)–(A8), and integrating over Φ , τ , and τ' , we finally get

$$\sigma = \Gamma(X \rightarrow 2\gamma) \frac{\alpha^2 m_x}{32E_0^4} \int \frac{d\omega}{\omega} FF', \quad (\text{A9})$$

where we use

$$F = \frac{1 + 2\tau_{\min}}{\tau_{\min}} \ln \frac{\tau_{\max}}{\tau_{\min}} - \frac{1}{\tau_{\min}} + \frac{1}{\tau_{\max}}, \quad (\text{A10})$$

with

$$\begin{aligned} \tau_{\min} &= \omega^2 / [4E_0(E_0 - \omega)], \\ \tau_{\max} &= \tau_{\min} + E_0(E_0 - \omega) \theta_{\max}^2 / (4m^2), \end{aligned} \quad (\text{A11})$$

and F' , τ'_{\min} , τ'_{\max} are defined in an analogous way, replacing ω by $\omega' = m_x^2/(4\omega)$.

For the integrated cross section of the complete process $e^-e^+ \rightarrow e^-e^+X \rightarrow e^-e^+\gamma\gamma$, we then get (using the fact that, in its rest frame, X decays isotropically into two photons)

$$\sigma = \frac{[\Gamma(X \rightarrow 2\gamma)]^2}{\Gamma(X \rightarrow \text{total})} \frac{\alpha^2 m_x}{32E_0^4} \int_{\omega_{\min}}^{\omega_{\max}} \frac{d\omega}{\omega} FF' \cos\psi_{\min}^*, \quad (\text{A12})$$

where ψ^* is defined as the emission angle of one of the real photons with respect to the $\gamma\gamma$ collision axis in the rest frame of X . In the approximation where this axis is identified with the e^-e^+ colliding-beam axis, one gets easily

$$\cos\psi_{\min}^* = \cos\psi_{\min} - \beta \frac{1 - \cos^2\psi_{\min}}{1 - \beta\cos\psi_{\min}}, \quad (\text{A13})$$

with

$$\beta = |m_x^2 - 4\omega^2| / (m_x^2 + 4\omega^2). \quad (\text{A14})$$

From (A13), it is readily shown that $\beta_{\max} = \cos\psi_{\min}$, whence it results that, because of the angular cutoff, the following minimal value is imposed on ω (and also on ω'):

$$\omega_{\min}^{(1)} = \frac{1}{2} m_x \tan \frac{1}{2} \psi_{\min}. \quad (\text{A15})$$

The symmetry existing between ω and $\omega' = m_x^2/(4\omega)$ allows us to rewrite (A12) in the form

$$\sigma = \frac{[\Gamma(X \rightarrow 2\gamma)]^2}{\Gamma(X \rightarrow \text{total})} \frac{\alpha^2 m_x}{16E_0^4} \int_{\omega_{\min}}^{\omega_{\max}} \frac{d\omega}{\omega} FF' \cos\psi_{\min}^*, \quad (\text{A16})$$

with

$$\omega_{\min} = \sup\{\omega_{\min}^{(1)}, \omega_{\min}^{(2)}, \omega_{\min}^{(3)}\}, \quad (\text{A17})$$

where one defines

$$\omega_{\min}^{(2)} = \chi_{\min} E_0, \quad \omega_{\min}^{(3)} = m_x^2 / (4\chi_{\max} E_0). \quad (\text{A18})$$

2. Background

Calling σ^{DB} the cross section for the double-bremsstrahlung diagram of Fig. 1(b), the Williams-Weizsäcker type of approximation we use, applied to the left-hand vertex, gives

$$\sigma^{\text{DB}} = \frac{\alpha}{4\pi E_0^2} \int \omega F \sigma^{\text{DC}}(\omega, E_0) d\omega, \quad (\text{A19})$$

where F is defined above in (A10), and $\sigma^{\text{DC}}(\omega, E_0)$ is the cross section for double Compton scattering between an "almost real" photon of energy ω and a positron of energy E_0 , colliding practically along the e^-e^+ colliding-beam axis.

From formula (11-31) of Ref. 21, we derive easily

$$\sigma^{\text{DC}} = \frac{\alpha^3}{32m^2 E_0 \omega} \int X E' dE' d(\cos\theta') d(\cos\psi^*), \quad (\text{A20})$$

where E' is the outgoing positron's energy and θ' its scattering angle (both in the lab frame); ψ^* is, in the c.m. frame of the outgoing photons, the angle of one of these photons with the "almost real" photon (ψ^* is thus defined as in part 1 above). The factor X , which contains the dynamics, is given by the formulas (11-33)–(11-35) of Ref. 22. Neglecting higher-order terms in m^2 and θ'^2 , and assuming $1/\psi^*$ to stay finite, we get

$$X = \frac{m^2}{2\omega^2} \left[\left(\frac{3 + \cos^2\psi^*}{\sin^2\psi^*} \right) u + \theta'^2 v \right], \quad (\text{A21})$$

with

$$u = \frac{m^2(E_0 - E')^4}{E_0^3 E'^3}, \quad v = \frac{E_0^2 + E'^2}{E_0 E'}. \quad (\text{A22})$$

After the trivial angular integrations, we obtain

$$\begin{aligned} \sigma^{\text{DC}} &= \frac{\alpha^3 \theta_{\max}^2}{128E_0 \omega^3} \\ &\times \int E' dE' \left[\frac{2(9 - \cos^2\psi_{\min}^*)u}{\sin^2\psi_{\min}^*} + \theta_{\max}^2 v \right] \cos\psi_{\min}^*. \end{aligned} \quad (\text{A23})$$

Using

$$E' = E_0 - \frac{M^2}{4\omega}, \quad dE' = \frac{M dM}{2\omega}, \quad (\text{A24})$$

where M^2 is the invariant mass squared of the outgoing photon pair, and substituting (A23) into (A19), we finally get

$$\sigma^{\text{DB}} = \frac{\alpha^4 \theta_{\text{max}}^2}{2^{10} \pi E_0^3} \int M dM \int \frac{d\omega}{\omega^3} F E' \cos \psi_{\text{min}}^* \times \left[\frac{2(9 - \cos^2 \psi_{\text{min}}^*) u}{\sin^2 \psi_{\text{min}}^*} + \theta_{\text{max}}^2 v \right], \quad (\text{A25})$$

where $\cos \psi_{\text{min}}^*$ is derived from (A13) and (A14) above, replacing m_X by M .

The numerical integration is then performed between the following limits:

$$M_{\text{min}} = m_X - \Delta m, \quad M_{\text{max}} = m_X + \Delta m, \quad (\text{A26})$$

$$\omega_{\text{min}} = \sup \{ \omega_{\text{min}}^{(1)}, \omega_{\text{min}}^{(2)}, \omega_{\text{min}}^{(3)} \}, \quad \omega_{\text{max}} = \frac{M^2}{4\omega_{\text{min}}}, \quad (\text{A27})$$

with

$$\omega_{\text{min}}^{(1)} = \frac{1}{2} M \tan \frac{1}{2} \psi_{\text{min}}, \quad \omega_{\text{min}}^{(2)} = \chi_{\text{min}} E_0, \quad \omega_{\text{min}}^{(3)} = \frac{M^2}{4\chi_{\text{max}} E_0}. \quad (\text{A28})$$

To include also the contribution of the symmetric diagram, we simply multiply formula (A25) by a factor of 2, neglecting the interference term between both diagrams. This procedure is justified, since, in the process represented by Fig. 1(b), the electron tends to lose much less energy than the positron [see the ω dependence in (A25)], whereas the opposite occurs in the symmetric process; thus the overlap between the final states of both processes should be very small.

*Work partly supported by the Commissariat à l'Énergie Atomique.

¹F. E. Low, Phys. Rev. **120**, 582 (1960). An improvement of this author's calculation was later given by J. C. Le Guillou, Compt. Rend. **261**, 326 (1965).

²H. Primakoff, Phys. Rev. **81**, 899 (1951).

³F. Calogero and C. Zemach, Phys. Rev. **120**, 1860 (1960).

⁴P. C. De Celles and J. E. Goehl, Jr., Phys. Rev. **184**, 1617 (1969).

⁵N. Arteaga-Romero, A. Jaccarini, and P. Kessler, Compt. Rend. **269B**, 153 (1969); **269B**, 1129 (1969); and Laboratoire de Physique Atomique Report No. PAM 70-02, 1970 (unpublished). A Jaccarini, N. Arteaga-Romero, J. Parisi, and P. Kessler, Lett. Nuovo Cimento **4**, 933 (1970); **1**, 935 (1971).

⁶V. E. Balakin, V. M. Budnev, and I. F. Ginsburg, ZhETF Pis. Red. **11**, 559 (1970) [Sov. Phys. JETP Lett. **11**, 388 (1970)].

⁷S. J. Brodsky, T. Kinoshita, and H. Terazawa, Phys. Rev. Letters **25**, 972 (1970); and Phys. Rev. D **4**, 1532 (1971). The latter paper contains also a study of $e^-e^+ \rightarrow e^-e^+X$ ($X = \pi^0, \eta$); however, no experimental cuts are accounted for in the numerical predictions.

⁸N. Arteaga-Romero, A. Jaccarini, P. Kessler, and J. Parisi, Phys. Rev. D **3**, 1569 (1971).

⁹J. Parisi, N. Arteaga-Romero, A. Jaccarini, and P. Kessler, Phys. Rev. D **4**, 2927 (1971).

¹⁰Actually, in our early papers of 1969, we chose a maximal e^\pm scattering angle $\theta_{\text{max}} = 3^\circ$. We were told afterwards by colliding-beam specialists (Professor Waloschek from DESY-Hamburg and Professor Haisinski from Orsay) that a value of a few milliradians (typically: 4 mrad) would be more realistic experimentally. On the other hand, such a small value is obviously preferable from the theoretical point of view, since it ensures that the virtual photons exchanged remain very near to their mass shell. It should also be stressed

that – because of the very sharp peaking of the scattering angle around 0° – the selection of such very small θ values does not involve an appreciable loss in the counting rates (as we have shown in Refs. 8 and 9).

¹¹B. Richter, in *Proceedings of the Fourteenth International Conference on High-Energy Physics, Vienna, 1968*, edited by J. Prentki and J. Steinberger (CERN, Geneva, 1968), pp. 13-14.

¹²Particle Data Group, Rev. Mod. Phys. **43**, S51 (1971).

¹³Particle Data Group, Rev. Mod. Phys. **43**, S66 (1971), and references quoted therein. It must be noticed that a very recent experiment performed at CERN [M. Basile *et al.*, Nuovo Cimento **3A**, 371 (1971)] led to a value about five times lower for this branching ratio. On the other hand, some theorists [see C. S. Lai, Nucl. Phys. **B14**, 348 (1969)] put the partial decay width $\Gamma(\eta' \rightarrow 2\gamma)$ much higher than our assumed value of 5 keV. One should remark (see Appendix of this paper) that our integrated cross section contains the product (branching ratio) \times (partial decay width).

¹⁴P. Kessler, Cahiers Phys. **20**, 55 (1966); Laboratoire de Physique Atomique Report No. PAM 68-05, 1968 (unpublished); Nucl. Phys. **B15**, 253 (1970).

¹⁵It may be noticed, for comparison, that the total cross sections (not accounting for any experimental cut) for the process $e^-e^+ \rightarrow e^-e^+X$ are: $\sigma = 5 \times 10^{-34} \text{ cm}^2$ for $X = \pi^0$, $E_0 = 1 \text{ GeV}$; $\sigma = 5 \times 10^{-34} \text{ cm}^2$ for $X = \eta$, $E_0 = 2 \text{ GeV}$; $\sigma = 4 \times 10^{-34} \text{ cm}^2$ for $X = \eta'$, $E_0 = 3 \text{ GeV}$. These predictions were obtained with a form factor of the dipole type for the $X\gamma\gamma$ vertices.

¹⁶Double-bremsstrahlung calculations have been performed by several authors, particularly in view of using this process for monitoring in electron-positron collisions. See, in particular, P. di Vecchia and M. Greco, Nuovo Cimento **50A**, 319 (1967), and references quoted therein. However, those authors' results cannot be used for the specific conditions we define in this paper.

¹⁷J. Parisi and P. Kessler, Lett. Nuovo Cimento **2**,

755 (1971).

¹⁸J. Lefrançois, Rapporteur's talk given at the International Symposium on Electron and Photon Interactions at High Energies, Cornell University, 1971 (unpublished).

¹⁹P. Lindenfeld, A. Sachs, and J. Steinberger, Phys. Rev. **89**, 531 (1953); C. P. Sargent, R. Cornelius, M. Rinehart, L. M. Lederman, and K. Rogers, Phys. Rev. **98**, 1349 (1955); Yu. A. Budagov, S. Wiktor, V. P. Dzhepelov, P. F. Ermolov, and V. I. Moskalev, Zh. Eksp. i Teor. Fiz. **38**, 1047 (1960) [Sov. Phys. JETP **11**, 755 (1960)]; N. P. Samios, Phys. Rev. **121**, 275 (1961); S. Devons, P. Nemethy, C. Nissim-Sabat, E. di Capua, and A. Lanzara, Phys. Rev. **184**, 1356 (1969).

²⁰J. Parisi, thèse de troisième cycle, Paris, 1970

(unpublished); J. Parisi and P. Kessler, in *Fourth International Symposium on Electron and Photon Interactions at High Energies, Liverpool, 1969*, edited by D. W. Braben and R. E. Rand (Daresbury Nuclear Physics Laboratory, Daresbury, Lancashire, England, 1970), p. 289; report, 1969 (unpublished); Lett. Nuovo Cimento **2**, 760 (1971).

²¹J. Parisi and P. Kessler, following paper, Phys. Rev. D **5**, 2237 (1972).

²²J. M. Jauch and F. Rohrlich, *The Theory of Photons and Electrons* (Addison-Wesley, Cambridge, Mass., 1955), p. 237. See also F. Mandl and T. H. R. Skyrme, Proc. Roy. Soc. (London) **A215**, 497 (1952).

PHYSICAL REVIEW D

VOLUME 5, NUMBER 9

1 MAY 1972

Investigation of the Vertices $\pi^0\gamma\gamma$, $\eta\gamma\gamma$, and $\eta'\gamma\gamma$ with Electron-Positron Storage Rings. II*

J. Parisi

Laboratoire de Physique Générale, Faculté des Sciences de l'Université VI de Paris, Paris, France

and

P. Kessler

Laboratoire de Physique Atomique, Collège de France, Paris, France

(Received 9 December 1971)

We here suggest an experimental investigation of the $X\gamma\gamma$ vertices ($X = \pi^0$, η , or η') in the specific case where both photons are spacelike, one of them being almost real and the other one highly virtual. For this purpose, we suggest that, in an electron-positron storage ring, e^-e^+ inelastic collisions of the type $e^-e^+ \rightarrow e^-e^+X \rightarrow e^-e^+\gamma\gamma$ should be analyzed, one of the outgoing e^\pm particles being detected at a very small scattering angle (a few milliradians), in coincidence with the other one measured at a relatively large scattering angle (higher than a few degrees) and with both decay photons emitted at large angle with respect to the beam axis. Assuming various experimental cutoffs on angles and energies, we show that (a) the background due to double bremsstrahlung can be made negligible through our choice of these cutoffs; (b) for $X = \pi^0$ or η , the cross sections should be high enough to justify experiments of this type to be planned with future storage rings of beam energy ≥ 3 GeV and luminosity $\geq 10^{32}$ cm⁻² sec⁻¹; (c) such experiments should allow a discrimination between various types of electromagnetic form factors used for the $X\gamma\gamma$ vertices.

I. INTRODUCTION

In a recent paper,¹ we suggested an investigation of the $X\gamma\gamma$ vertices ($X = \pi^0$, η , η') in electron-positron storage rings, using the process $e^-e^+ \rightarrow e^-e^+X \rightarrow e^-e^+\gamma\gamma$ under specific experimental conditions which should be the following: Both outgoing e^\pm particles would be detected at very small scattering angles, in coincidence with both photons produced at large angles with respect to the beam axis. Such an experiment should allow a quite precise measurement of the various $X\gamma\gamma$ coupling constants [or, equivalently, of the decay widths $\Gamma(X \rightarrow 2\gamma)$]. This suggestion inserted itself into the general scheme defined in our previous papers^{2,3}

for studying photon-photon collisions through inelastic e^-e^+ scattering processes (and in particular reactions of the type $e^-e^+ \rightarrow e^-e^+A^-A^+$, where A^\pm is any charged particle) in electron-positron colliding-beam devices.

We here suggest the following variant of the experimental scheme proposed before: Only one of the outgoing e^\pm particles would be detected at a very small scattering angle (not more than a few milliradians), whereas the other one would be measured at a relatively large scattering angle (at least a few degrees). Thus, only one of the virtual spacelike photons exchanged [see the Feynman diagram of Fig. 1(a)] would be almost real [its q^2 value would be lower than a few (MeV/c)² for beam